Supplementary Information

Viscosity Prediction of CO_2-Saturated Imidazolium-Based Ionic Liquids Using ε^*-Modified Sanchez–Lacombe Equation of State and Free Volume Theory with a New Correction Term

Ryohei Otani,[a] Yuya Hiraga,[a,*] Masaru Watanabe[a,**]
[a] Research Center of Supercritical Fluid Technology, Tohoku University Aramaki Aza Aoba 6-6-11, Aoba-ku, Sendai, Miyagi 980-8579, Japan

*Corresponding author. E-mail: yuya.hiraga.d6@tohoku.ac.jp (Y. Hiraga).

**Corresponding author. E-mail: masaru.watanabe.e2@tohoku.ac.jp (M. Watanabe).

S1 Calculation for pure IL density

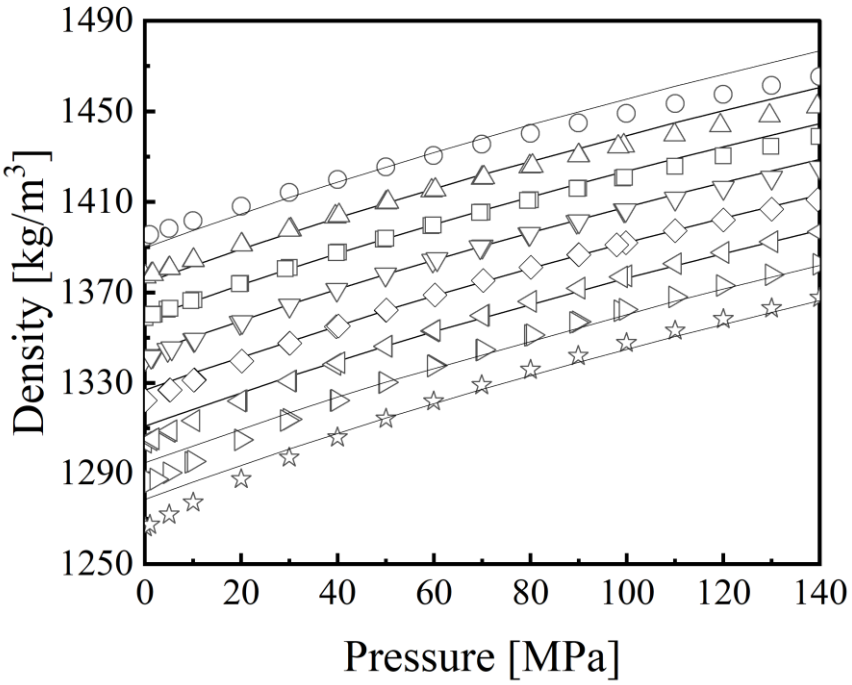

Fig. S1 Correlation results for the density of [hmim][Tf_2N]. Symbols: ○, 273 K; △, 293 K; □, 313 K; ▽, 333 K; ◇, 353 K; ◁, 373 K; ▷, 393 K; ☆, 413 K.[1] Lines: ε^*-mod SL-EoS.

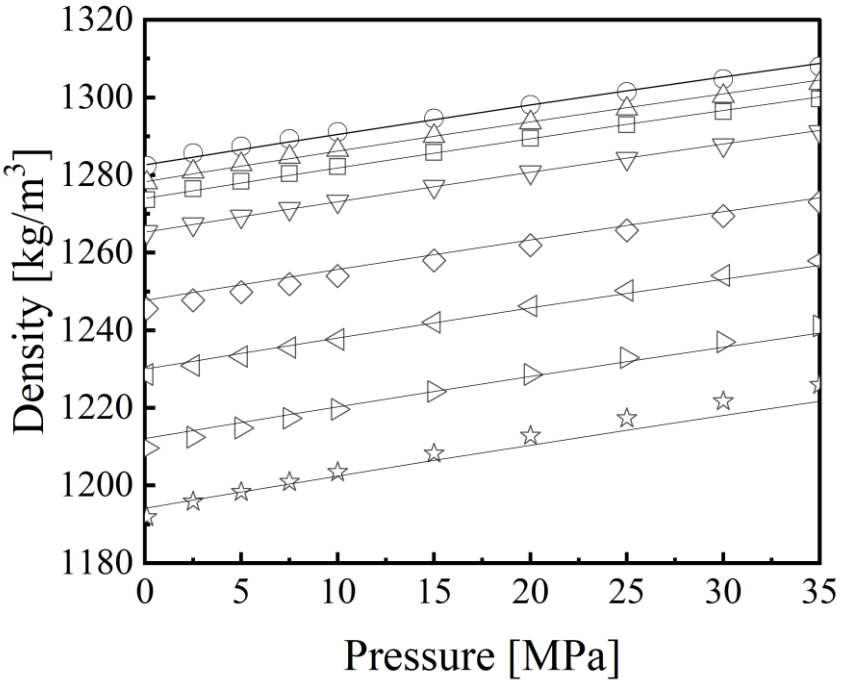

Fig. S2 Correlation results for the density of [dmim][Tf_2N]. Symbols: ○, 293 K; △, 298 K; □, 303 K; ▽, 313 K; ◇, 333 K; ◁, 353 K; ▷, 373 K; ☆, 393 K.[2] Lines: ε^*-mod SL-EoS.

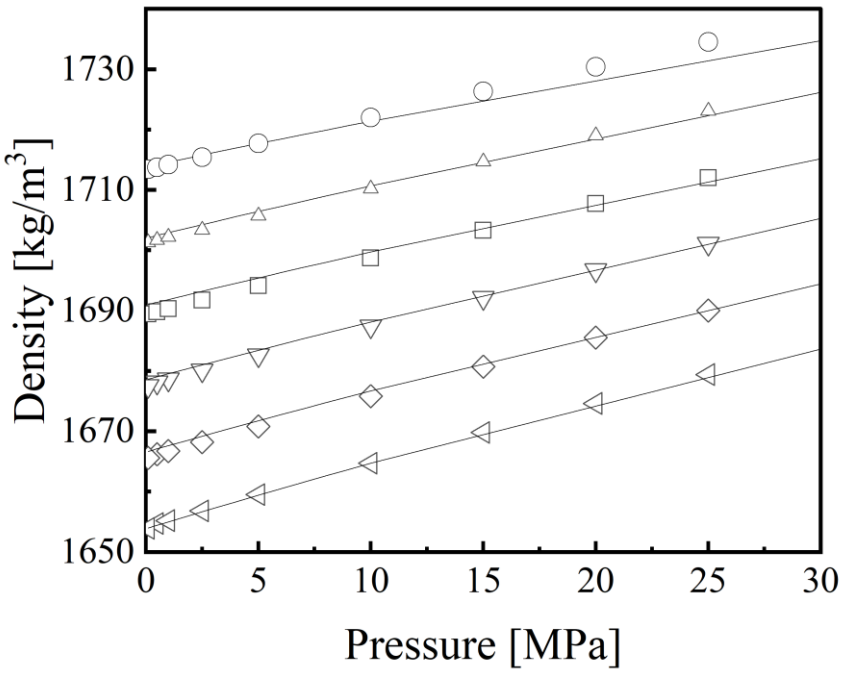

Fig. S3 Correlation results for the density of [emim][FAP]. Symbols: ○, 293 K; △, 303 K; □, 313 K; ▽, 323 K; ◇, 333 K; ◁, 343 K.[3] Lines: ε^*-mod SL-EoS.

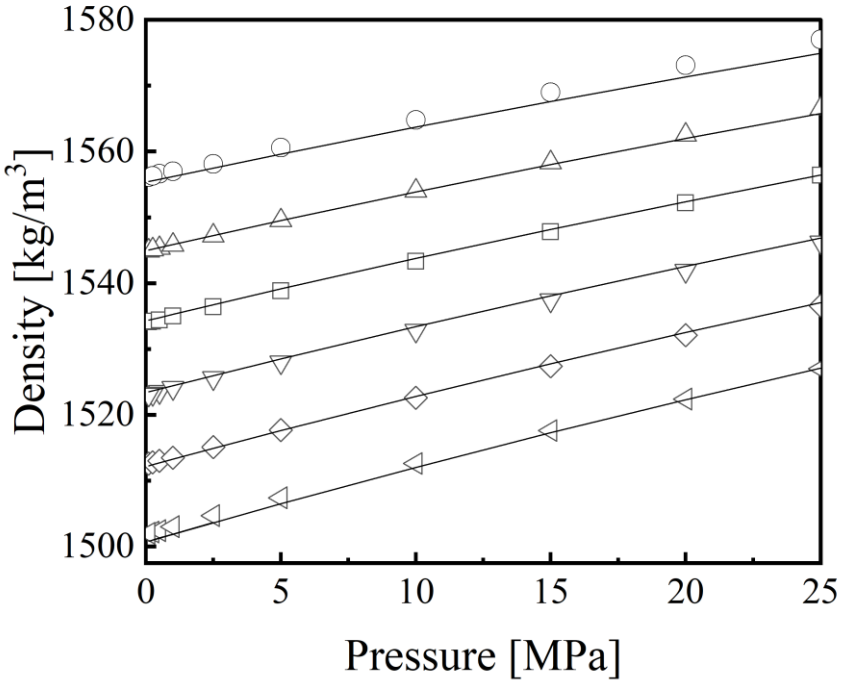

Fig. S4 Correlation results for the density of [hmim][FAP]. Symbols: ○, 293 K; △, 303 K; □, 313 K; ▽, 323 K; ◇, 333 K; ◁, 343 K.[3] Lines: ε^*-mod SL-EoS.

S2 Calculation for pure IL viscosity

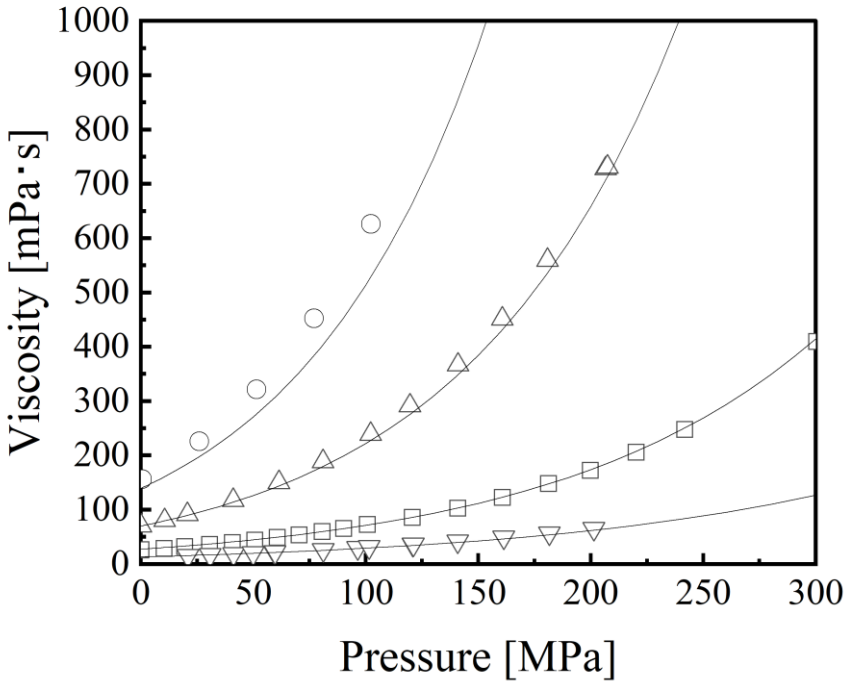

Fig. S5 Correlation results for viscosity of [hmim][Tf_2N]. Symbols: ○, 283.15 K; △, 298.15 K; □, 323.15 K; ▽, 348.15 K.[4] Lines: FVT + ε^*-mod SL-EoS.

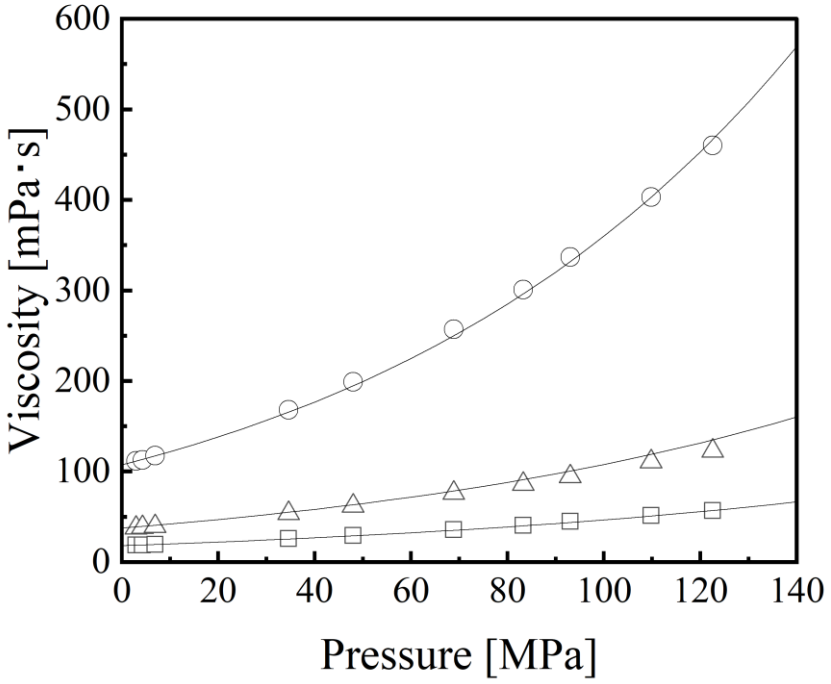

Fig. S6 Correlation results for viscosity of [dmim][Tf_2N]. Symbols: ○, 298.15 K; △, 323.15 K; □, 343.15 K.[5] Lines: FVT + ε^*-mod SL-EoS.

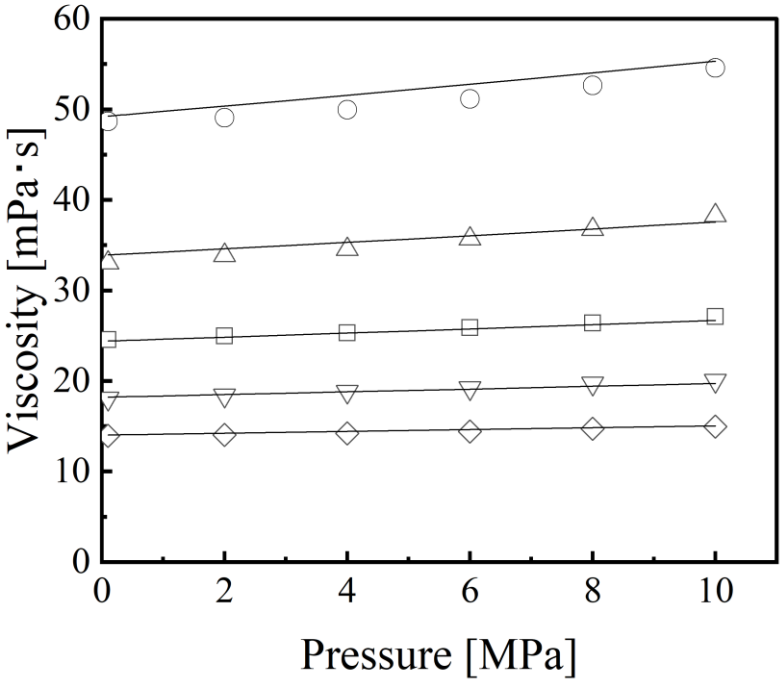

Fig. S7 Correlation results for viscosity of [emim][FAP]. Symbols: ○, 303.15 K; △, 318.15 K; □, 323.15 K; ▽, 333.15 K.[6] Lines: FVT + ε^*-mod SL-EoS.

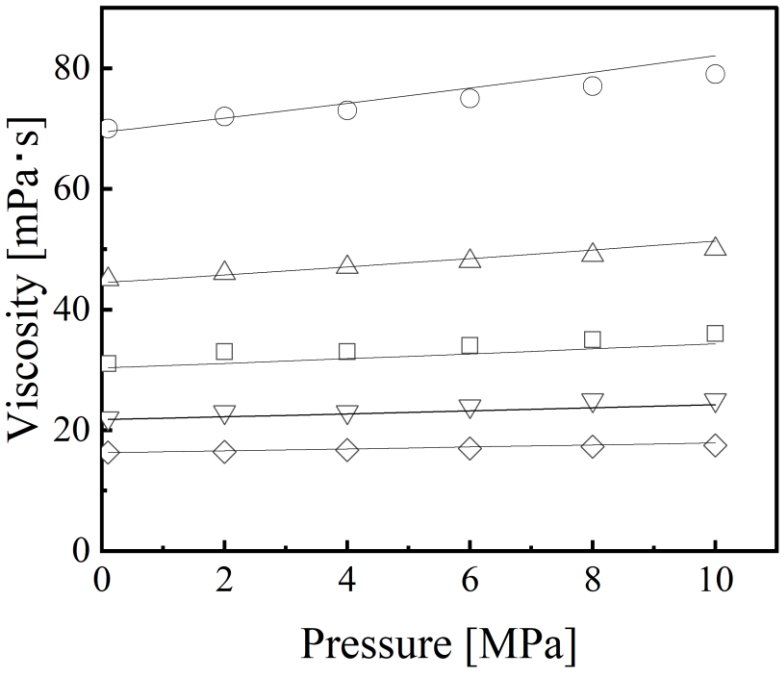

Fig. S8 Correlation results for viscosity of [hmim][FAP]. Symbols: ○, 303.15 K; △, 318.15 K; □, 323.15 K; ▽, 333.15 K.[6] Lines: FVT + ε^*-mod SL-EoS.

S3 Calculation for CO_2 solubility

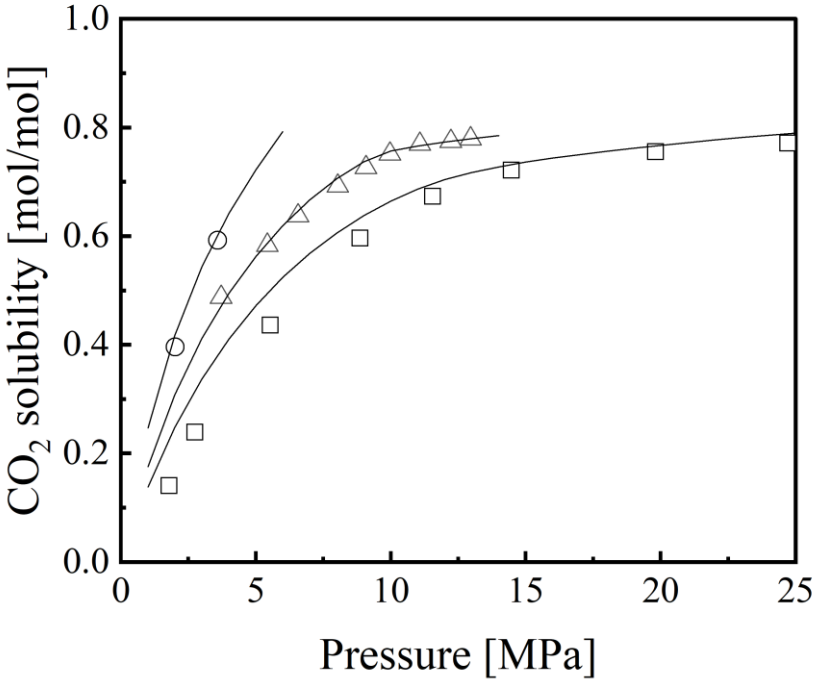

Fig. S9 Correlation results for CO_2 solubility in [hmim][Tf_2N]. Symbols: ○, 298.15 K; △, 323.15 K; □, 343.15 K.[7] Lines: FVT + ε^*-mod SL-EoS.

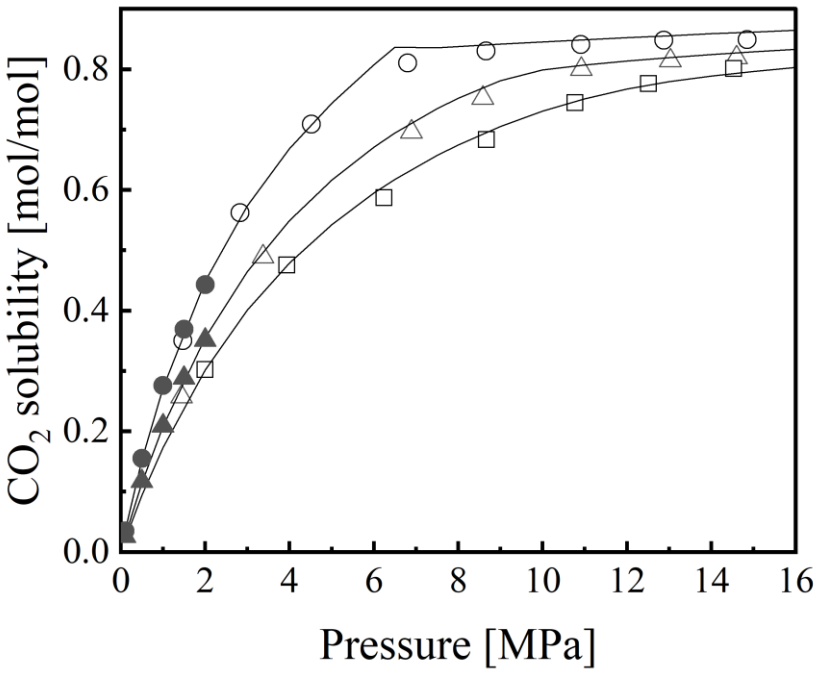

Fig. S10 Correlation results for CO_2 solubility in [dmim][Tf_2N]. Symbols: ○, 298.15 K;[7] ●, 298.15 K;[8] △, 323.15 K;[7] ▲, 323.15 K;[8] □, 343.15 K.[7] Lines: FVT + ε^*-mod SL-EoS.

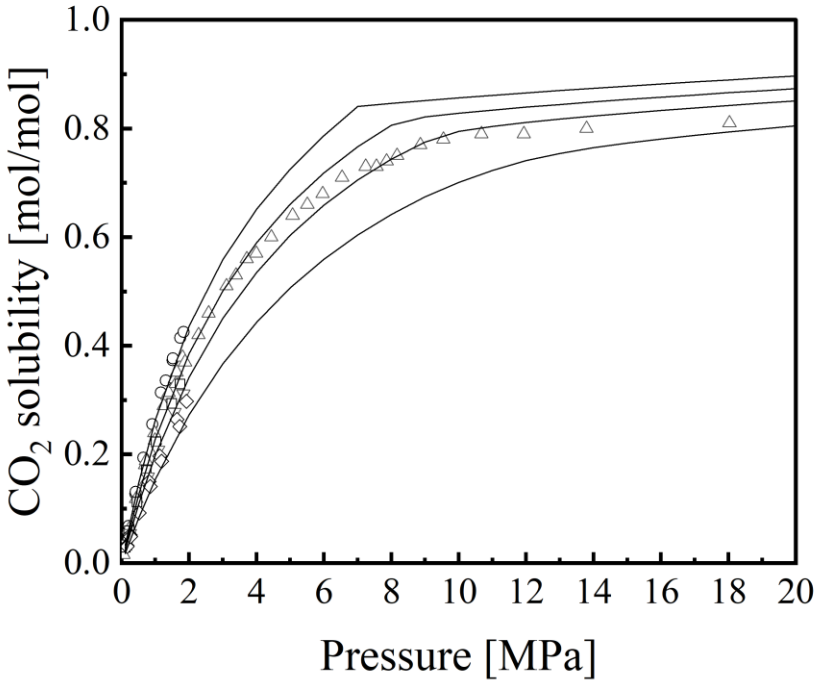

Fig. S11 Correlation results for CO_2 solubility in [emim][FAP]. Symbols: ○, 303.15 K; △, 313.15 K; □, 323.15 K; ▽, 343.15 K.[9] Lines: FVT + ε^*-mod SL-EoS.

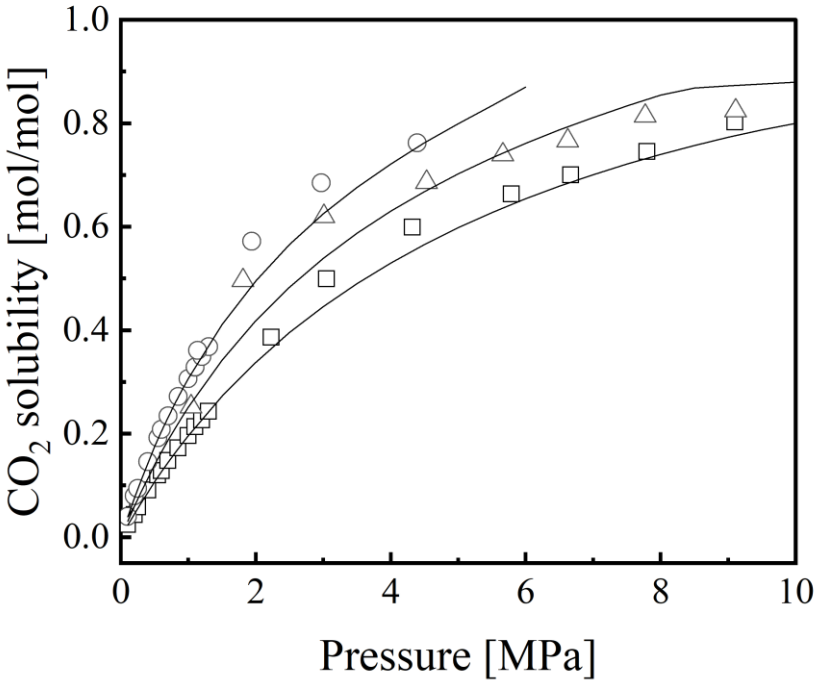

Fig. S12 Correlation results for CO_2 solubility in [hmim][FAP]. Symbols: ○, 298.15 K; △, 313.15 K; □, 333.15 K.[10] Lines: FVT + ε^*-mod SL-EoS.

S4 Viscosity of IL + CO_2 mixtures using β determined by correlation

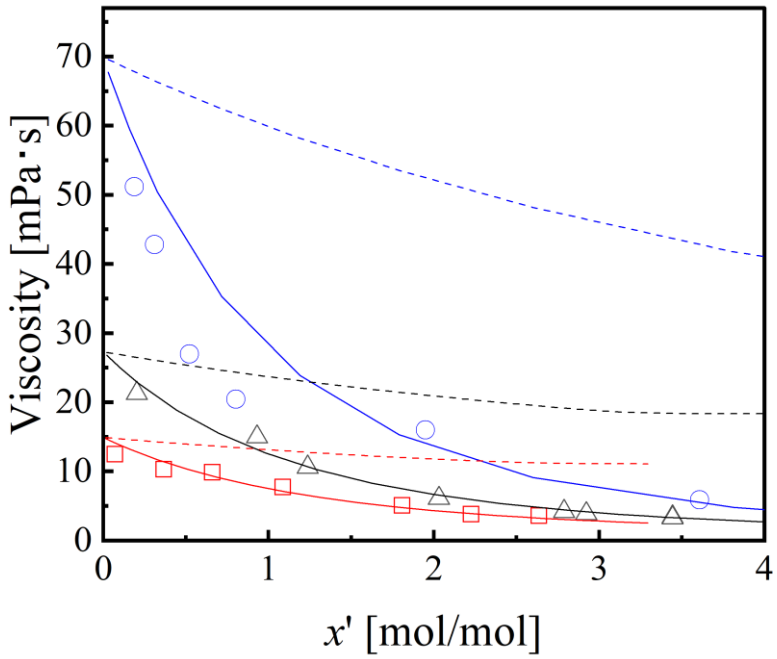

Fig. S13 Prediction and correlation results for the viscosity of the [hmim][Tf_2N] + CO_2 mixture. Symbols: ○, 298.15 K; △, 323.15 K; □, 343.15 K.[11] Dashed lines: Prediction with FVT + ε^*-mod SL-EoS ($\beta = 0$). Solid lines: Correlation with FVT + ε^*-mod SL-EoS ($\beta \neq 0$).

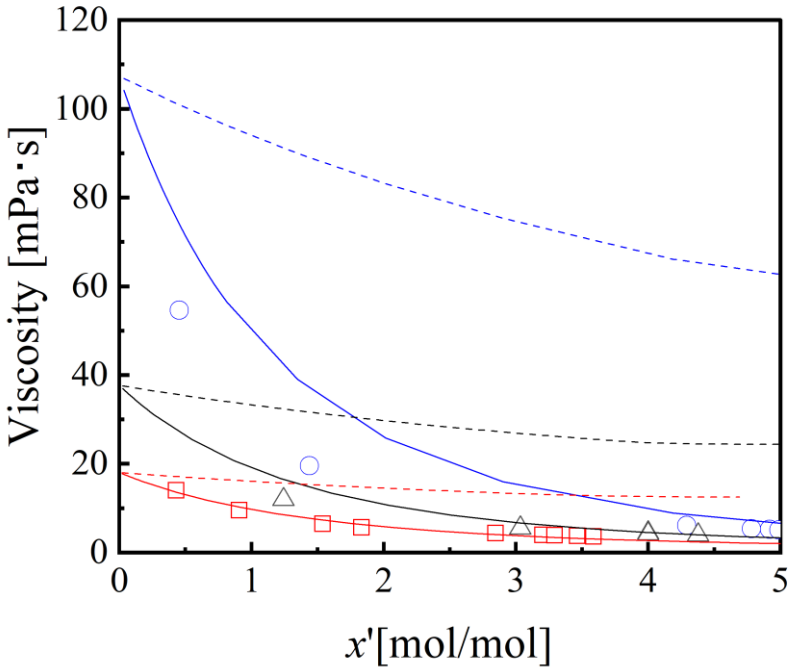

Fig. S14 Prediction and correlation results for the viscosity of the [dmim][Tf_2N] + CO_2 mixture. Symbols: ○, 298.15 K; △, 323.15 K; □, 343.15 K.[11] Dashed lines: Prediction with FVT + ε^*-mod SL-EoS ($\beta = 0$). Solid lines: Correlation with FVT + ε^*-mod SL-EoS ($\beta \neq 0$).

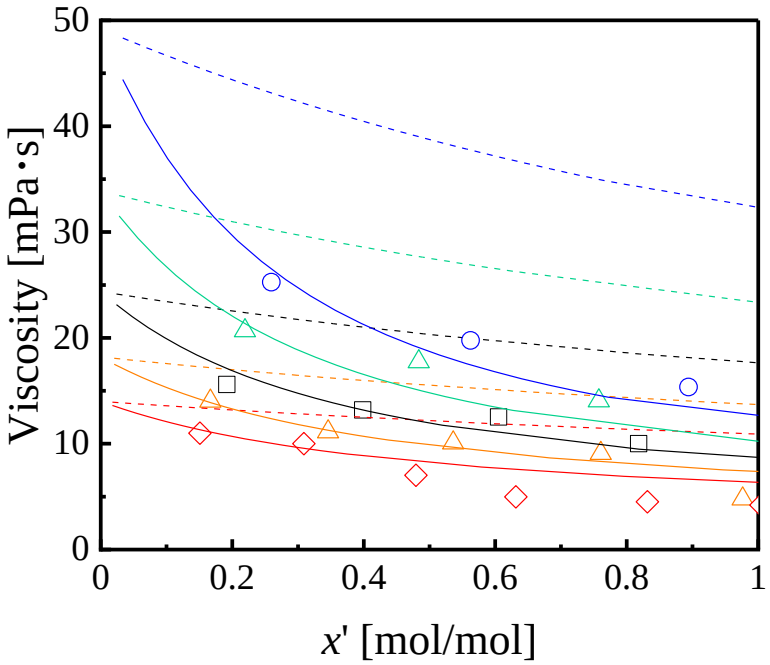

Fig. S15 Prediction and correlation results for the viscosity of the [emim][FAP] + CO_2 mixture. Symbols: ○, 293.15 K; △, 313.15 K; □, 323.15 K; ▽, 333.15 K; ◇, 343.15 K.[6] Dashed lines: Prediction with FVT + ε^*-mod SL-EoS ($\beta = 0$). Solid lines: Correlation with FVT + ε^*-mod SL-EoS ($\beta \neq 0$).

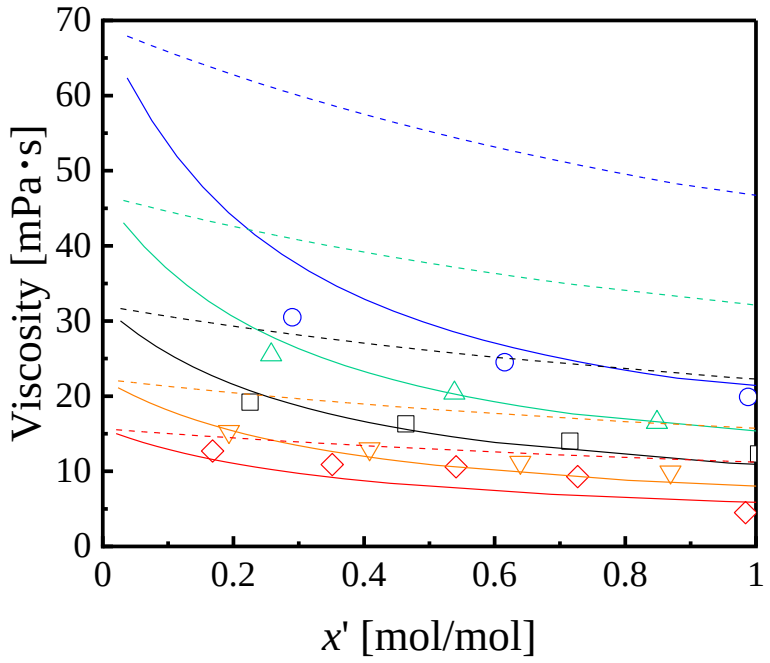

Fig. S16 Prediction and correlation results for the viscosity of the [hmim][FAP] + CO_2 mixture. Symbols: ○, 293.15 K; △, 313.15 K; □, 323.15 K; ▽, 333.15 K; ◇, 343.15 K.[6] Dashed lines: Prediction with FVT + ε^*-mod SL-EoS ($\beta = 0$). Solid lines: Correlation with FVT + ε^*-mod SL-EoS ($\beta \neq 0$).

S5 Viscosity of IL + CO_2 mixtures using β predicted by solubility parameters

The solubility parameters were calculated based on the following method with reference to the literature.[12] The solubility parameter of CO_2, δ_{CO_2}, was calculated using the Span and Wagner equation[13] and following equation (Eq. (S1)).

$$\delta_{CO_2} = \left(\rho \cdot \left(\widehat{U}^0(\rho^0, T) - \widehat{U}(\rho, T)\right)\right)^{\frac{1}{2}} \quad \text{(S1)}$$

The $\widehat{U}^0$ represents the internal energy in the ideal gas state at ρ =0.1kg/m^3, and $\widehat{U}$ represents the internal energy at the temperature and pressure of the system.

The method for calculating the solubility parameter of the ionic liquid, δ_{IL}, is as follows. First, the critical constants and acentric factor of the ionic liquid were calculated using the group contribution method by Valderrama.[14] Then, these values were applied to the Pitzer correlation to determine the enthalpy of vaporization ΔH.[15] The molar volume V_{m} was calculated using the molar mass and the density at 298 K and 0.1 MPa. Finally, these parameters were substituted into Eq. (S2) to calculate δ_{IL}.

$$\delta_{IL} = \left(\frac{\Delta H - RT}{V_{\mathrm{m}}}\right)^{\frac{1}{2}} \quad \text{(S2)}$$

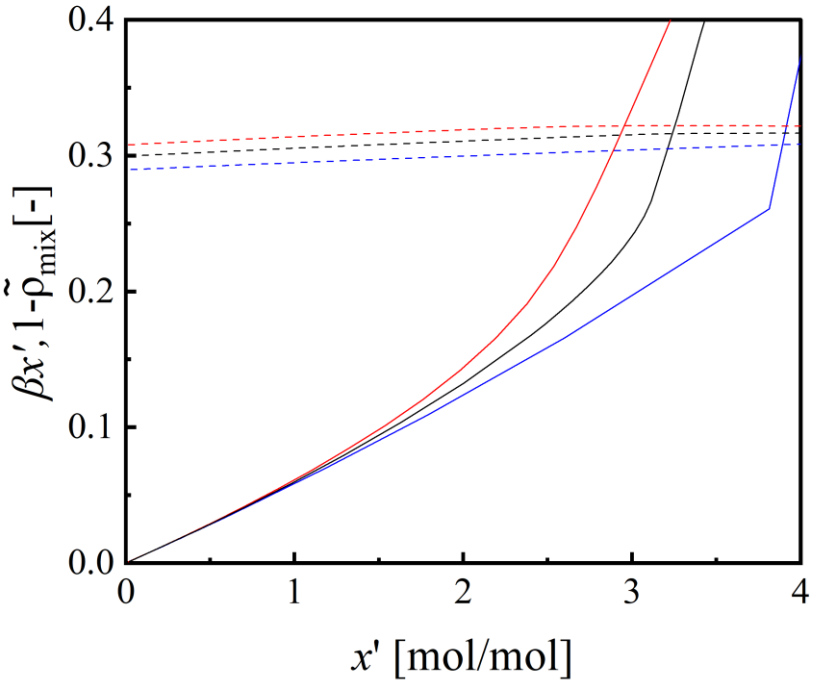

Fig. S17 Contribution of "1- $\tilde{\rho}_{mix}$ " (Dashed lines) and " $\beta x'$ " (Solid line) of [hmim][Tf_2N] + CO_2 mixture. Lines; blue, 298.15 K; black, 323.15 K; red, 343.15 K.

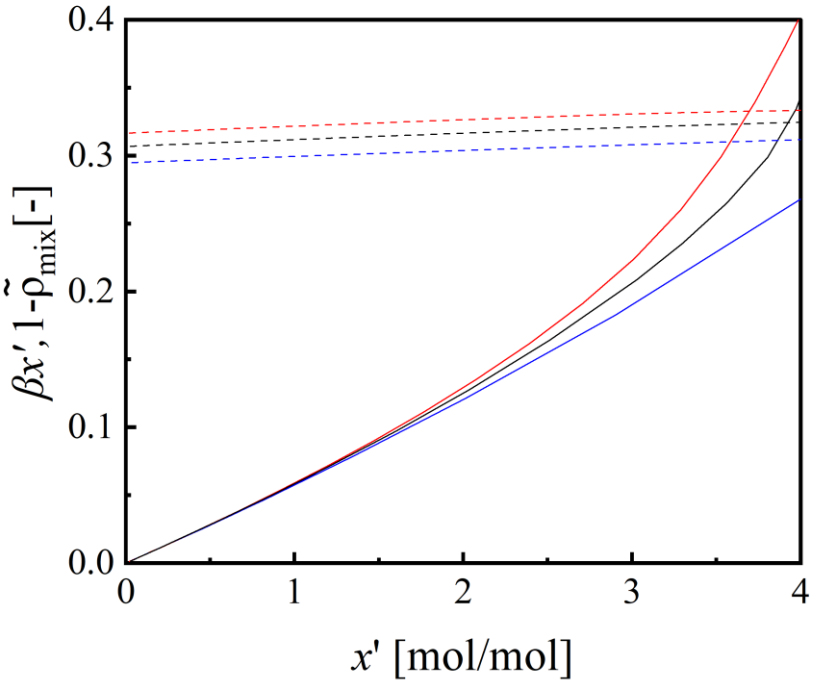

Fig. S18 Contribution of "1- $\tilde{\rho}_{mix}$ " (dashed lines) and " $\beta x'$ " (solid lines) of [dmim][Tf_2N] + CO_2 mixture. Lines; blue, 298.15 K; black, 323.15 K; red, 343.15 K.

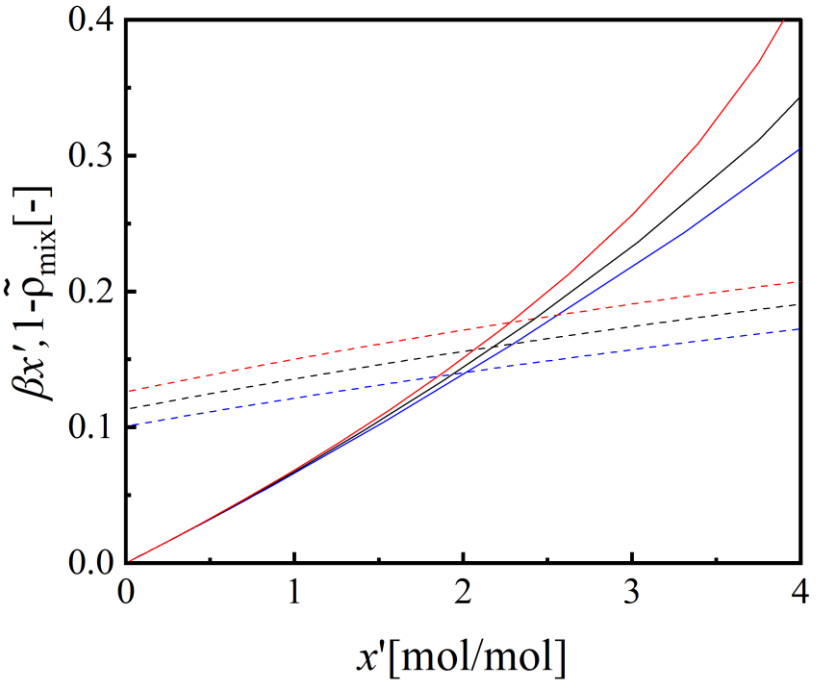

Fig. S19 Contribution of "1- $\tilde{\rho}_{mix}$" (dashed lines) and "$\beta x'$" (solid line) of [hmim][FAP] + CO_2 mixture. Lines; blue, 303.15 K; black, 323.15 K; red, 343.15 K.

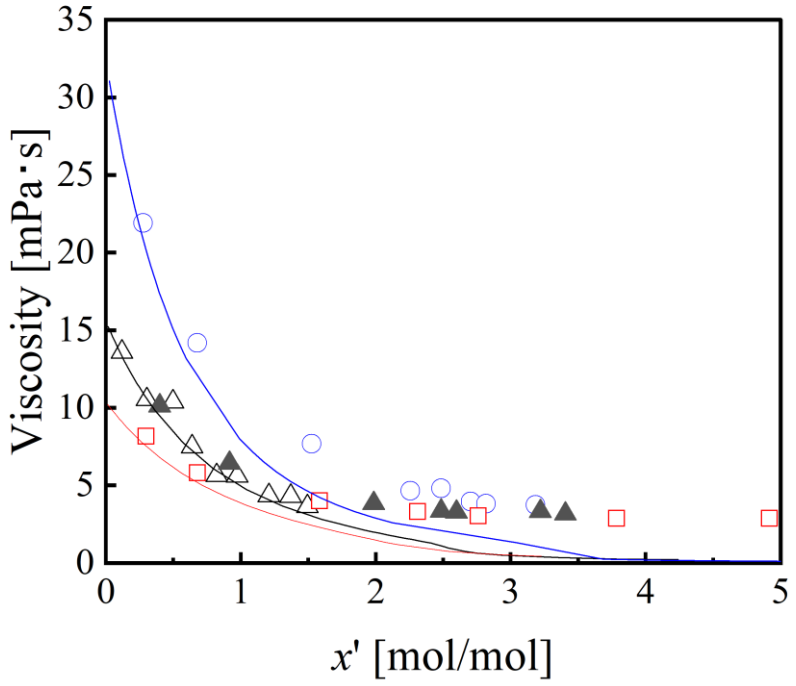

Fig. S20 Prediction results using solubility parameters for the viscosity of [emim][Tf_2N] + CO_2 mixture. Symbols: ○, 298.15 K; △, 323.15 K; □, 343.15 K[11]; ▲, 323.15 K.[6] Solid lines: Prediction with FVT + ε^*-mod SL-EoS.

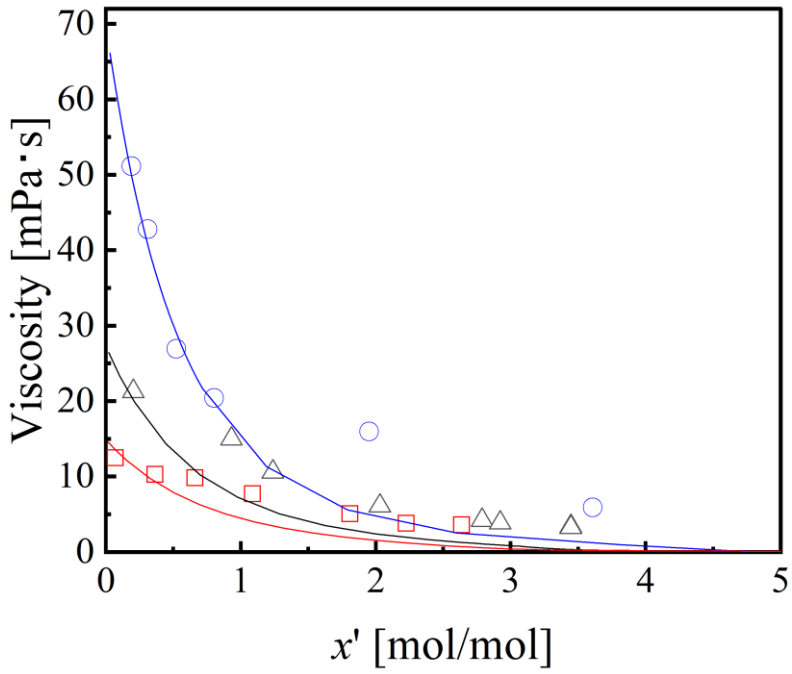

Fig. S21 Prediction results using solubility parameters for the viscosity of [hmim][Tf_2N] + CO_2 mixture. Symbols: ○, 298.15 K; △, 323.15 K; □, 343.15 K.[11] Solid lines: Prediction with FVT + ε^*-mod SL-EoS.

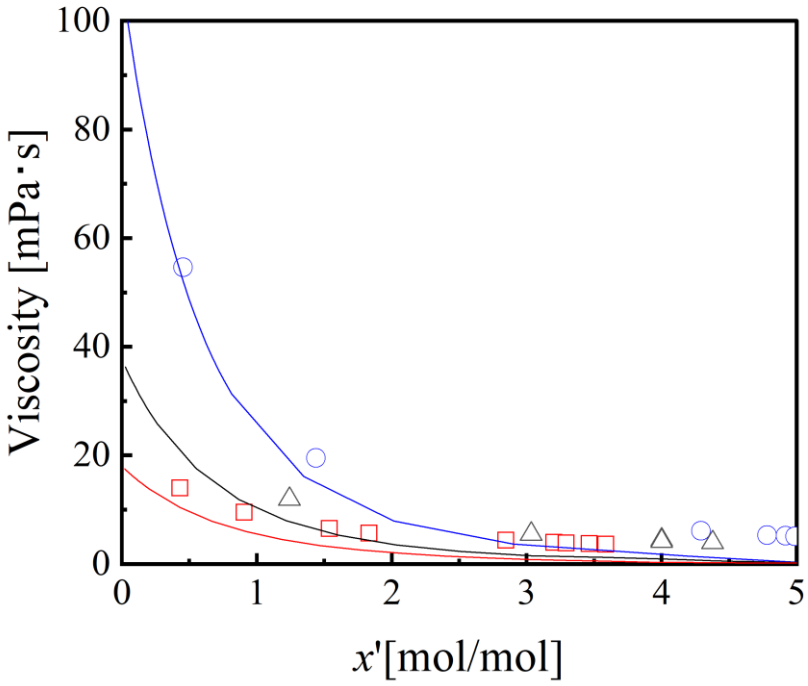

Fig. S22 Prediction results using solubility parameters for the viscosity of [dmim][Tf_2N] + CO_2 mixture. Symbols: ○, 298.15 K; △, 323.15 K; □, 343.15 K.[11] Solid lines: Prediction with FVT + ε^*-mod SL-EoS

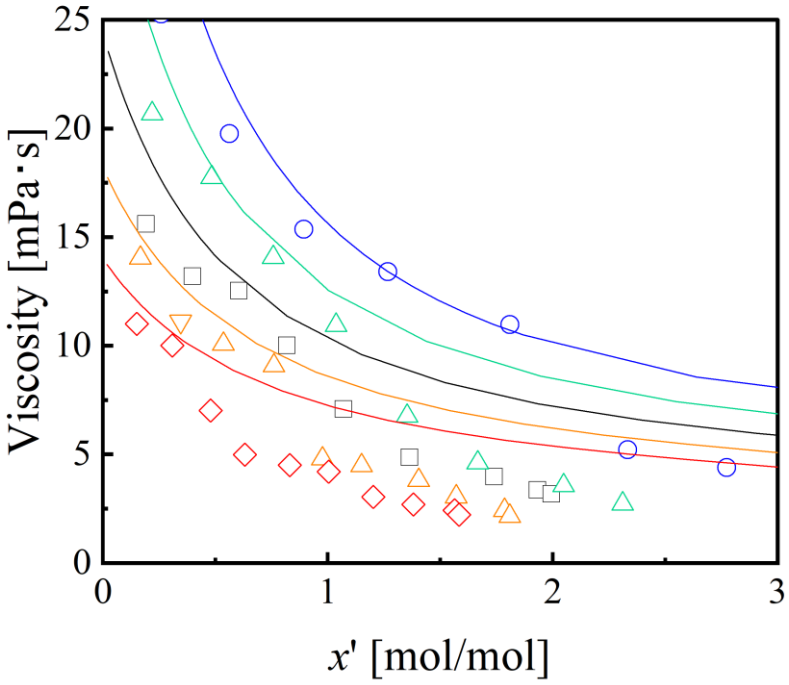

Fig. S23 Prediction results using solubility parameters for the viscosity of [emim][FAP] + CO_2 mixture. Symbols: ○, 293.15 K; △, 313.15 K; □, 323.15 K; ▽, 333.15 K; ◇, 343.15 K.[6] Solid lines: Prediction with FVT + ε^*-mod SL-EoS.

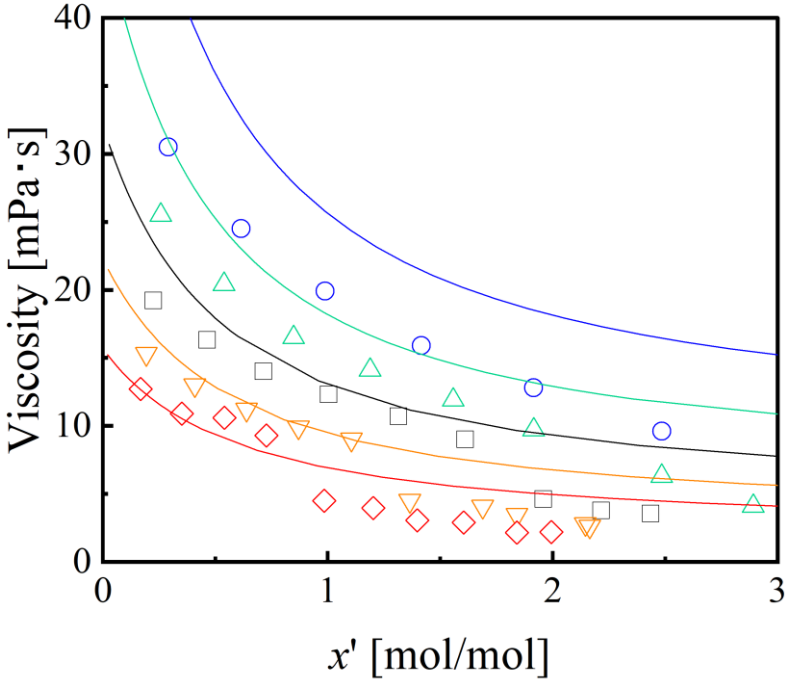

Fig. S24 Prediction results using solubility parameters for the viscosity of [hmim][FAP] + CO_2 mixture. Symbols: ○, 293.15 K; △, 313.15 K; □, 323.15 K; ▽, 333.15 K; ◇, 343.15 K.[6] Solid lines: Prediction with FVT + ε^*-mod SL-EoS.

References

1. J. Safarov, R. Hamidova, S. Zepik, H. Schmidt, I. Kul, A. Shahverdiyev and E. Hassel, *J. Mol. Liq.*, 2013, **187**, 137-156.
2. L. I. N. Tomé, P. J. Carvalho, M. G. Freire, I. M. Marrucho, I. M. A. Fonseca, A. G. M. Ferreira, J. o. A. P. Coutinho and R. L. Gardas, *J. Chem. Eng. Data*, 2008, **53**, 1914-1921.
3. D. Almantariotis, S. Stevanovic, O. Fandino, A. S. Pensado, A. A. Padua, J. Y. Coxam and M. F. Costa Gomes, *J. Phys. Chem. B*, 2012, **116**, 7728-7738.
4. K. R. Harris and M. Kanakubo, *J. Chem. Eng. Data*, 2021, **66**, 4618-4628.
5. A. Ahosseini and A. M. Scurto, *Int. J. Thermophys.*, 2008, **29**, 1222-1243.
6. K. Li, W. Wu, L. Peng and H. Zhang, *J. Mol. Liq.*, 2021, **337**, 116240.
7. W. Ren, B. Sensenich and A. M. Scurto, *J. Chem. Thermodyn.*, 2010, **42**, 305-311.
8. M. Gonzalez-Miquel, J. Bedia, J. Palomar and F. Rodriguez, *J. Chem. Eng. Data*, 2014, **59**, 212-217.
9. A. H. Jalili, M. Shokouhi, G. Maurer and M. Hosseini-Jenab, *J. Chem. Thermodyn.*, 2013, **67**, 55-62.
10. M. J. Muldoon, S. N. V. K. Aki, J. L. Anderson, J. K. Dixon and J. F. Brennecke, *J. Phys. Chem. B*, 2007, **111**, 9001-9009.
11. A. Ahosseini, E. Ortega, B. Sensenich and A. M. Scurto, *Fluid Phase Equilib.*, 2009, **286**, 72-78.
12. Y. Hiraga, W. Endo, H. Machida, Y. Sato, T. M. Aida, M. Watanabe and R. L. Smith Jr, *J. Supercrit. Fluids*, 2012, **66**, 49-58.
13. R. Span and W. Wagner, *J. Phys. Chem. Ref. Data*, 1996, **25**, 1509-1596.
14. J. O. Valderrama, L. A. Forero and R. E. Rojas, *Ind. Eng. Chem. Res.*, 2012, **51**, 7838-7844.
15. B. E. Poling, R. C. Reid, J. M. Prausnitz and J. P. O'Connell, *The Properties of Gases and Liquids*, McGraw-Hill, New York, 5th edn., 2001.